In vitro study of a standardized approach to aortic cusp extension

Riccardo Vismara[1,3], Alberto M. Leopaldi[1,3], Claudia Romagnoni[2,3], Monica Contino[2,3], Andrea Mangini[1,2,3], Marco Stevanella[1,3], Gianfranco B. Fiore[1,3], Carlo Antona[2,3]

[1] Department of Electronic, Information and Bioengineering, Politecnico di Milano, Milan - Italy
[2] Cardiovascular Surgery Department, Luigi Sacco University General Hospital, Milan - Italy
[3] For Cardio Lab, Università di Milano - Politecnico di Milano, Milan - Italy

INTRODUCTION

Aortic valve (AV) reparative surgery techniques aim at restoring valve function by preserving the original anatomical structures as much as possible (1-3). The advantages of valve repair with respect to valve replacement are well acknowledged, but the complexity of the procedures and the lack of standardization have hindered the spread of the reparative approach (4-8).

The AV cusp extension technique (CET), which was first described by Duran and colleagues (9), consists in restoring proper leaflet coaptation by suturing pericardium patches to the native leaflets. This technique can be used for AV repair whenever a cusp retraction or loss of tissue is present, e.g. for rheumatic valves, congenital diseases, endocarditis, leaflets perforations, and annulus dilatation (9-12). The extending patches are meant to recreate a functional morphology of the valve, improving its coaptation reserve. Despite being one of the most long-standing reparative techniques described, CET is still far from being standardized.

Indeed, no univocal agreement on the optimal graft shape and patch sizing emerges from ananalysis of the literature

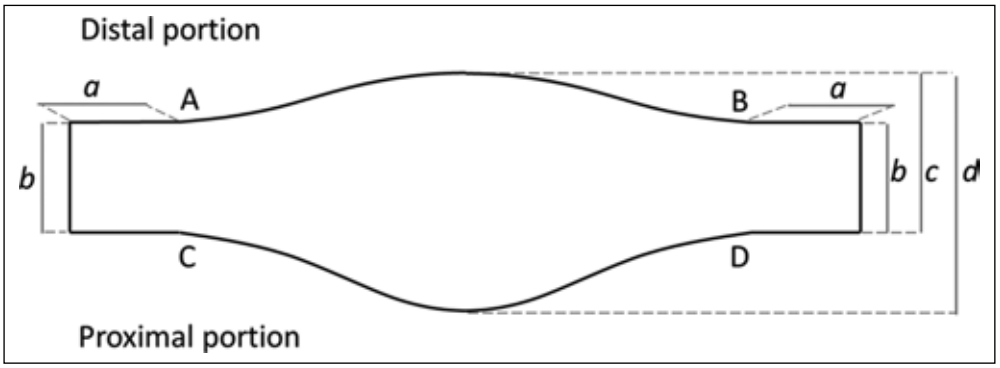

Fig. 1 - *Schematic representation of a BPP.* ***AB:*** *free edge (from 18 to 42 mm, step 2 mm).* ***CD:*** *proximal portion.* ***a, b:*** *lateral appendages (5 x 5 mm).* ***c:*** *height of the coaptation portion (6 mm).* ***d:*** *total patch height (10 mm).*

(11-15). The evaluation of these crucial aspects is entirely demanded of the surgeon, who has to dimension and shape the cusp extensions in the operating room on the sole basis of a visual inspection of the unloaded AV.

In this work we describe an *in vitro* study of a novel approach to CET, in which standard pre-cut pericardium patches are prepared in multiple sizes and implanted by the surgeon according to the specific patient anatomy. In order to enhance standardization and reproducibility (16-18), a geometrical model of the AV was used to aid the size decision-making process of the surgeon. Validation was carried out on swine AV samples using a state-of-the-art *in vitro* mock loop, analyzing the standard hydrodynamic and kinematic evaluation indexes.

MATERIALS AND METHODS

CET methodology

Our approach to CET was characterized by two main features, as described in the following: i) the use of standardized, pre-built pericardium patches; and ii) the choice of the patch size to be implanted by means of a simple geometrical model of the AV, which correlated in each cusp the intercommissural distance (i.e., the distance between the commissures of the cusp) with the length of the corresponding free edge (FE), which is the length of the rim running from commissure to commissure and passing through the nodulus of Arantius.

Pericardium patch geometry

A set of pre-built bovine pericardium patches (BPP), with differing free edge lengths (from 18 to 42 mm, step 2 mm), was developed. The bovine pericardium was prepared according to the protocol proposed by Santibáñez (19). Figure 1 shows a scheme of a BPP with the relevant dimensions. The shape and the dimensions of the BPP were derived from surgical and anatomical considerations, as well as from the literature. The total height of the patch (Fig. 1d) was fixed to 10 mm, while the height of the coapting portion (Fig. 1c) was fixed to 6 mm in order to provide satisfying coaptation (11, 13). Each patch was provided with two additional lateral appendages (Fig. 1, a = 5 mm, b = 5 mm) that were tied to the aortic wall at the commissural level to stabilize the patch in place. The proximal profile (Fig. 1CD) replicates the typical shape of the cusp after pathological tissue has been removed and, if needed, might be adapted by the surgeon to best fit the specific leaflet condition. The distal profile (Figure 1AB), whose length is proportional to the FE length, replicates the one proposed by Kalangos (11) and is tangential to the lateral appendages. Patch thickness, evaluated with a micrometer (Metrica., Milan, Italy), was 0.52 ± 0.14 mm.

Geometrical model for the patch size choice

In order to guide in the choice of the appropriate set of BPPs, a geometrical model of the AV was developed (Appendix A). The model correlated the three inter-commissural distances, measured by the surgeon in the operating room by means of compasses, with the FE of each cusp, whose correct dimensioning is crucial for AV continence. Since every pre-cut BPP features a specific FE length, the model is used to determine the appropriate set of three cusp-specific patches that should be sutured to restore proper leaflet coaptation.

Surgical technique

The surgical technique for the BPPs was as follows (11). Each patch was sutured to the aortic wall with a 2-0 braided suture, tied outside the aorta wall and reinforced with two pledgets on the external and internal sides of the aortic wall. Each patch was sutured to the free edge of each native cusp with a running 5-0 polypropylene non-everting mattress suture, starting from the midpoint of the cusp, up to the commissures.

In vitro experimental campaign

Mock loop

Figure 2 gives a schematic of the experimental setup. The mock loop consisted in a pulsatile, computer-controlled, piston pump, a housing section for the AV sample, and an adjustable hydraulic afterload that simulated the systemic hydraulic impedance (20, 23, 24). The loop was equipped for pressure measurement with three piezoresistive pressure transducers (140 PC series; Honeywell, Morristown, NJ, USA), two of which were placed immediatelly upstream from (P_{ven}) and downstream of (P_{ao}) the AV, and the third was placed in the systemic impedance simulator (P_{art}). Flow through the AV was measured with a transit-time flow meter (HT110R; Transonic Systems, Ithaca, NY, USA) placed downstream from the AV (Q). High speed videos (1000 fps) of the aortic view of the valve were recorded with a digital camera (Phantom Miro2; Vision Research, Wayne, NJ, USA).

Experimental protocol

Seven AV samples were harvested by experienced surgeons from fresh swine hearts obtained from the local abattoir (swine weighed 162 ± 10 kg). The samples were prepared to be housed in the mock loop as previously described (20): the ascending aorta was trimmed 15 mm above the sinotubular junction, the outflow tract of the left ventricle was reconstructed suturing the anterior mitral leaflet to the paravalvular structures, and coronary ostia were ligated to avoid fluid loss. Valve diameter, evaluated by a go no-go gauge, was 23 ± 2.1 mm. The sample was then housed in the mock loop and tested in basal conditions (70 bpm, with 80 mL of stroke volume). After each sample was tested in its physiologic condition,

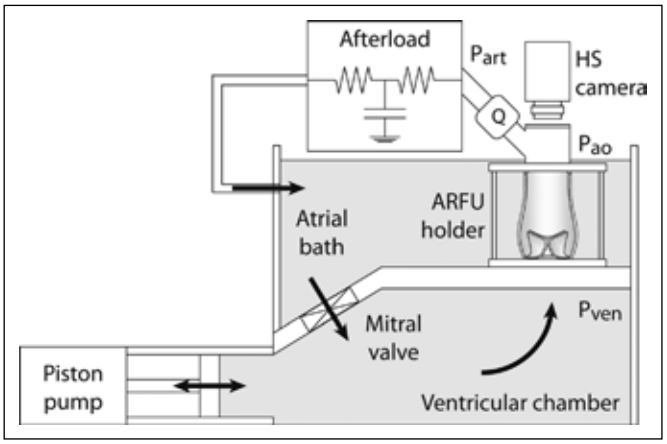

Fig. 2 - *Mock loop scheme. AV = aortic valve; HS camera = high speed camera; P_{ven} = ventricular pressure. P_{ao} = aortic pressure. P_{art} = simulated arterial pressure. Q = aortic flow.*

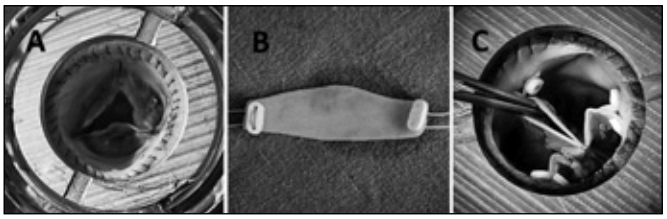

Fig. 3 - *Main steps of the CET procedure.* ***(A)*** *AV insufficiency is induced on the sample by removing a lens-shape portion of tissue from each cusp.* ***(B)*** *Picture of the BPP to be implanted.* ***(C)*** *Aortic valve after CET was performed.*

AV insufficiency was generated by the surgeon cutting a lens-shaped portion of tissue from each cusp, 8 mm to 10 mm in height, mimicking cusp retraction or damage. In panel A of Figure 3, the AV with induced insufficiency is shown. The three inter-commissural distances were evaluated by the surgeon with compasses, and the appropriate extensions (Fig. 3B) were chosen using the geometrical model. CET was then applied (Fig. 3C) and the sample was tested in the mock loop again. For both the physiologic and after-surgery conditions, the following data were analyzed.

Data processing

Hydrodynamics

Pressure curves upstream and downstream of the sample were acquired, together with flow rate. Raw data were

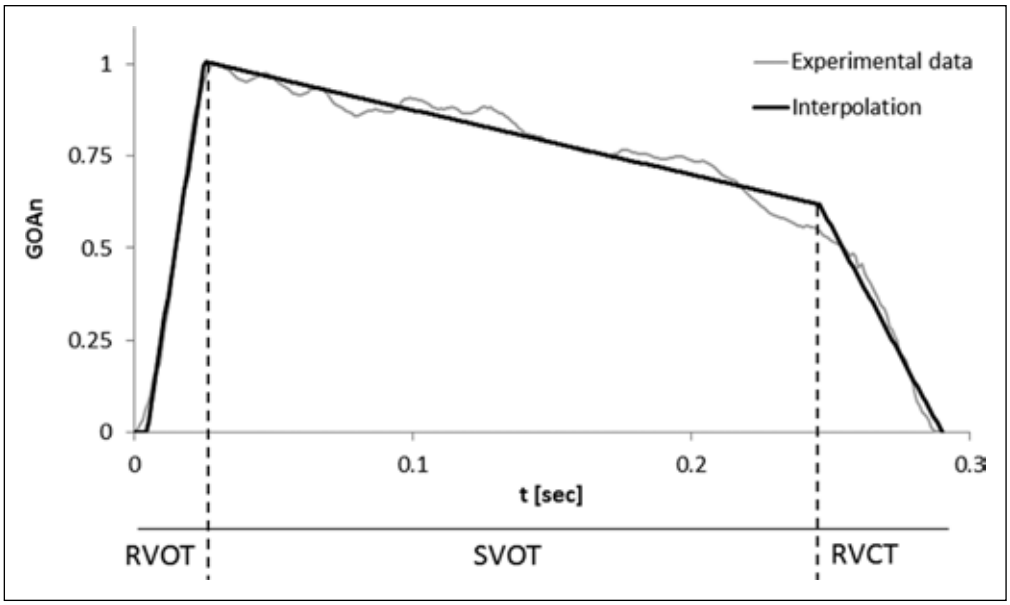

Fig. 4 - *Opening and closing phases. Interpolation of the experimental data. RVOT = rapid valve opening time; SVOT = slow valve opening time; RVCT = rapid valve closing time.*

sampled at 1000 Hz and recorded. From these data the following quantities were evaluated:

- P_{art} [mmHg], mean simulated arterial blood pressure.
- SV [mL], stroke volume.
- Q [l/min], mean flow rate.
- SRF [%], static regurgitant fraction (the percent volume of fluid flowing back while the valve is in its fully closed diastolic configuration; SRF was evaluated as reported in Vismara et al (21)).
- CV [mL], closing volume (evaluated as the time integral of the first negative flow peak after the end of the systole).
- Δp_{mean} [mmHg], mean systolic pressure drop across the sample.
- Δp_{max} [mmHg], maximum systolic pressure drop.
- $Ed_{sys\%}$, energy dissipated during the systole (% of the energy transferred by the pump in the simulated cycle)
- $Ed_{dia\%}$, energy dissipated during the diastole (% of the energy transferred by the pump in the simulated cycle)

Kinematics

Leaflet kinematics was evaluated from the high speed movies extracting the time course of the two-dimensional geometric orifice area (GOA). To this purpose, an in-house code was implemented in MATLAB (The Math Works, Natick, MA, USA) to automatically identify and segment, using a region-growing method, the valvular orifice in each frame of three consecutive cardiac cycles. The time course of the GOA in such three cycles was subsequently averaged and normalized, thus obtaining for each tested valve a single curve [of normalized GOA (GOA_n)] ranging from 1 (maximum valve opening) to 0 (closed valve). By adapting the approach described by Leyh and colleagues (25) for echocardiography data, three distinct phases of the ejection time (ET) motion were identified and quantified as:

- Rapid valve opening time (RVOT)
- Slow valve closing time (SVCT)
- Rapid valve closing time (RVCT)

The estimation of RVOT, SVCT, and RVCT was performed through a least-squares approach, minimizing the residuals between the experimental GOA_n data and the following system of equations, where t_{RVO}, t_{SVC}, and t_{RVC} are the time instants at which the rapid valve opening, the slow valve closing and the rapid valve closing respectively end:

$$GOA_n(t) = \frac{GOA_n(t_{RVO})}{t_{RVO} - t_0} t = \frac{GOA_n(t_{RVO})}{RVOT} t \qquad for\ t \le t_{RVO}$$

$$GOA_n(t) = \frac{GOA_n(t_{SVC}) - GOA_n(t_{RVO})}{t_{SVC} - t_{RVO}} t = \frac{GOA_n(t_{SVC}) - GOA_n(t_{RVO})}{SVCT} t \qquad for\ t_{RVO} \le t \le t_{SVC}$$

$$GOA_n(t) = \frac{-GOA_n(t_{SVC})}{t_{RVC} - t_{SVC}} t = \frac{-GOA_n(t_{SVC})}{RVCT} t \qquad for\ t_{SVC} \le t \le t_{RVC}$$

by best-fitting the values of t_0, t_{RVO}, $GOA_n(t_{RVO})$, t_{SVC}, $GOA_n(t_{SVC})$ and t_{RVC}. Figure 4 shows a representative example of the interpolation of the experimental data.

Statistical analysis

For each sample, hydrodynamic data were averaged on five consecutive cycles. Gaussian distribution was tested using the Shapiro-Wilk test. In case of normality, data were presented as means ± standard deviations and Student's paired *t*-test was used to calculate p. If normality was not verified, data were presented as median, 25° and 75° percentile and the Mann-Whitney rank sum test was used to calculate p. In both cases, a two-tailed p value <0.05 was considered statistically significant.

RESULTS

Hydrodynamic results are reported in Table I. No statistically significant difference was observed between the mock loop working parameters (P_{art}, SV) pre- and post-treatment, thus demonstrating the reproducibility of the experimental test conditions. An increase in Δp_{mean} (from 1.7 ± 0.9 mmHg to 3.1 ± 1.3 mmHg, p<0.05) was observed after CET, while the minor change observed for Δp_{max} (from 24.0 ± 5.6 mmHg to 25.4 ± 5.0 mmHg) was not statistically significant. Moreover, both SRF and CV increased after CET (from 3.5 ± 2.4% to 6.9 ± 2.7% and from 4.7 ± 0.6 to 7.0 ± 1.5 mL, p<0.05), leading to a decrease in mean flow rate (from 4.8 ± 0.4 to 4.4 ± 0.4 l/min, p<0.05) in the post-surgery samples. The $Ed_{dia\%}$ changed accordingly, shifting from 5.8 ± 1.7% to 9.0 ± 1.8% (p<0.05), while the variation in $Ed_{sys\%}$ (from 2.2 ± 1.0% to 3.4 ± 2.0%) was not statistically significant.

TABLE I - HYDRODYNAMIC INDEXES IN BASAL CONDITION AND AFTER SURGERY

	Basal	CET	*P*
P_{art} [mmHg]	92.9 (90.8-106.4)	92.7 ± 5.0	0.34
SV [mL]	74.9 ± 6.3	74.0 ± 6.1	0.09
Q [l/min]	4.8 ± 0.4	4.4 ± 0.4	<0.05
SRF [%]	3.5 ± 2.4	6.9 ± 2.7	<0.05
CV [mL]	4.7 ± 0.6	7.0 ± 1.5	<0.05
Δp_{mean} [mmHg]	1.7 ± 0.9	3.1 ± 1.3	<0.05
Δp_{max} [mmHg]	24.0 ± 5.6	25.4 ± 5.0	0.10
$Ed_{sys\%}$ [%]	2.2 ± 1.0	3.4 ± 2.0	0.05
$Ed_{dia\%}$ [%]	5.8 ± 1.7	9.0 ± 1.8	<0.05

CET = cusps extension technique; P_{art} = mean simulated arterial blood pressure; SV = stroke volume; Q = mean flow rate; SRF = static regurgitant fraction; CV = closing volume; Δp_{mean} and Δp_{max} = mean and maximum pressure drop across the valve; $Ed_{sys\%}$ and $Ed_{dia\%}$ = dissipated energy during the systole and the diastole.

TABLE II - KINEMATIC INDEXES OBTAINED THROUGH HS VIDEO, IN BASAL CONDITION AND AFTER SURGERY

	Basal	CET	*P*
ET [ms]	290 ± 13	310 ± 19	<0.05
RVOT [ms]	18 ± 3	18 ± 4	0.86
SVCT [ms]	203 ± 8	200 ± 20	0.63
RVCT [ms]	68 ± 7	92 ± 24	<0.05

CET = cusp extension technique; ET = ejection time; RVOT = rapid valve opening time; SVCT = slow valve closing time; RVCT = rapid valve closing time.

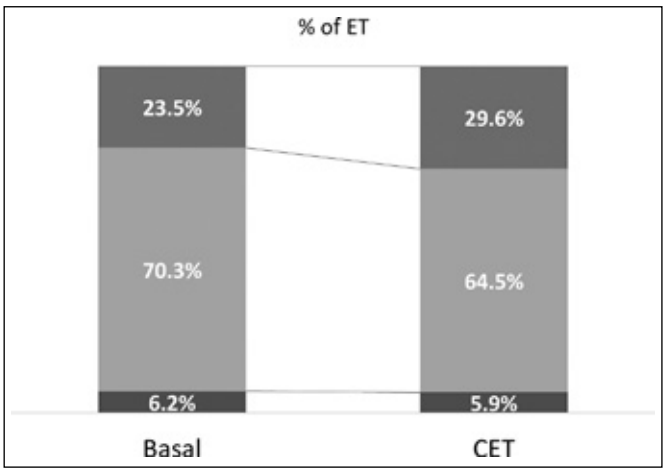

Fig. 5 - *Opening and closing phases as a percentage of the ejection time (ET) in Basal and CET treated samples. RVOT = rapid valve opening time; SVCL = slow valve closing time; RVCT = rapid valve closing time.*

Table II shows the kinematic parameters. CET altered the valve ET (from 290 ± 13 ms to 310 ± 19 ms, p<0.05). This increase was mainly due to an altered closing kinematics, particularly to variations of the rapid closing phase. Indeed, RVCT augmented from 68 ± 7 ms to 92 ± 24 (p<0.05) while the other phases were only slightly altered by the surgery. Figure 5 exemplifies these alterations as percent values of the ETs.

DISCUSSION

The reparative surgery for the treatment of AV insufficiency showed encouraging results in terms of freedom from

reoperation (4, 5) and several advantages as compared to valve replacement (6, 7). Although in recent years the growing understanding of AV functioning has contributed to boosting this approach, its level of acceptance by the cardiac surgeon community is still far from that of mitral valve repair techniques (8). One of the primary causes for this lack of acceptance probably lies in the complexity and operator-dependence of the reparative surgical acts, when compared to valve replacement (2, 8, 11). In order to overcome these drawbacks, standardization of reparative approaches is strongly needed in order to obtain more predictable and reliable clinical outcomes, to help surgeons in their surgical interventions, and to simplify their training and learning process.

Among the reparative approaches to AV insufficiency, CET is one of the most complex and is currently applied with durable results (11-15) in case of severe cusp retraction or in case of congenital AV disease in young patients. In the present work we developed and tested a standardized, simplified surgical strategy for cusp extension in the case of tricuspid aortic valves. Our approach provided the surgeon with standard pre-cut patches, whose leaflet-specific sizes were selected using a geometrical model of the AV, thus reducing the surgeon's burden of choice in the procedure. The results of our experimental campaign indicated that CET performed with this approach induces only slight alterations in the hemodynamics and in the kinematics of the AV *in vitro*.

The tailoring of the leaflet patches is a crucial step of the reparative procedure, directly affecting the final outcome of the surgery. With the usual methodology, the surgeon has to evaluate the anatomy of the diseased valve and has to infer the correct shape and dimensions of the patches in order to obtain proper coaptation of the repaired valve. Obviously, this step is highly subjective, which makes the surgery outcome extremely operator-dependent. In order to help the surgeon in this process, we proposed a two-fold innovation with respect to the state of the art: the use of standard pre-built BPPs, made available with different FE lengths, and the use of a geometrical model to select the best triplet of leaflet-specific patches to be implanted. The former feature helps reduce the surgical time and the subjectivity of the procedure, potentially encouraging its diffusion. Secondly, the choice of the patches is aided by the use of an objective geometrical model, whose inputs are the three inter-commissural distances that can be promptly measured in the OR with a standard compass. In particular, the model encompasses a simplified 3D reconstruction of the AV in which, rather than assuming axial symmetry, leaflets with different sizes are considered. In this way, with simple assumptions and by elementary trigonometric calculations, it is possible to directly relate the three inter-commissural distances to the three leaflet-free edges. This provides the indications for a set of optimal, geometrically self-compatible patches to be sutured.

The efficacy and reliability of this methodology was verified *in vitro* by comparing the hemodynamic and kinematic behavior of the repaired valve with the native physiological one. CET induced a statistically significant increase in the mean trans-valvular pressure drop, while peak pressure drop increase was not statistically significant. In any case, none of these quantities reached clinically relevant values as a consequence of CET, and these values were far below those previously measured with a state-of-the-art commercial bioprosthesis that was tested in the same *in vitro* setup (21). Reasonably, the alterations in these hemodynamic parameters were caused by the different geometrical and mechanical properties of the pericardium patches with respect to natural valve leaflets. In particular, the cusps are taller after CET in consideration of the 5 mm portion of the patch that is sewed to the aortic wall. Moreover, it is realistic to expect that the greater stiffness of the pericardium patches compared to the natural cusp tissue (26) may cause some increased hydrodynamic hindrance to the systolic flow.

Concerning valve competence, the SRF increased after valve repair as compared to the one measured in physiologic samples; nonetheless, this increment should not be interpreted as an indication of a surgery-induced valve insufficiency. In our *in vitro* investigation, the post-surgery sample was not compared to an insufficient valve, but to an 'ideal' comparison term, i.e., a physiological, perfectly continent valve. Therefore, the SRF measured under basal conditions should be interpreted as a bias introduced by the *in vitro* system, which is mainly related to the measuring approach (21). Similarly, the post-surgery increase in SRF was reasonably caused by the leaks induced by stitches on the valve leaflets. Indeed, CET requires the execution of multiple sutures which, in the absence of blood coagulation, may result in small, yet significant, fluid losses.

As concerns AV kinematics, the ejection time increased after surgery, owing to a slower rapid-closing phase. This result is consistent with the statistically significant increase of the valve closing volume, and may be related to complex

biomechanical interplays between the valve structures and the fluid. Indeed, since the valve is a totally passive structure, its kinematics are only driven by hydrodynamic quantities, and they are affected by the inertial mass of the cusps, which is altered by CET. This may result in a slowdown of the cusp movements, which our results suggest to be more relevant in the rapid closing phase, whose duration increased significantly after surgery. Interestingly, no such effects were recorded in the valve opening phase, probably because of the impulsive nature of this phase. In other words, the sudden temporal changes of the local hemodynamic quantities that occur at the early systolic thrust play a major role in determining the opening kinematics, which may mask, to a certain extent, the effects of increased tissue inertia.

Study limitations

In this study both the experimental and the geometrical model of the AV are healthy, thus limiting the clinical applicability of the experimental results. We performed CET on healthy AV after the excision of the central portion of each cusp, so to reproduce the ideal morphology of the incontinent valve for rheumatic disease after the surgical excision of the diseased tissues. Therefore, our results might be more significant with reference to patients with AV insufficiency secondary to severe cusp retraction and with no structural anomalies of the AV.

The proposed approach cannot take into account any kind of remodeling processes of the valve over time. Most of all, it cannot conveniently apply to bicuspid-AV affected patients as well as to young patients with congenital defects of the AV, who are also ideal candidates for AV repair techniques. In this cohort of patients, the anatomical peculiarities of the AV demands *ad hoc* developed geometrical models, while an *in vitro* study is practically unfeasible. In this context, experimental limitations might be overcome by resorting to computational analyses, namely developing a FEM model based on previously developed AV models (27, 28), which, once validated on the basis of the results of this work, could be conveniently used in a systematic study of CET applied to AV with congenital diseases.

The aortic root dimensions were evaluated as they are in an operating room, i.e., with the aortic root cut open and with the aortic valve in unloaded conditions. The rationale of this choice lies in an attempt to replicate the real scenario the surgeon has to face in the experimental campaign, and to enhance the repeatability of the measurements. This approach leads to a bias in estimating the dimensions of the aortic root in loaded conditions. In the future, we plan to overcome this limit by using a FEM approach to investigate the effects exerted by aortic root compliance on root geometry over the cardiac cycle.

CET was performed only with home-cured bovine pericardium, since the focus of the study was the surgical technique rather than the material. Nevertheless, the mid- to long-term results of this fixed pericardium in CET performance are under debate, with some authors reporting lower freedom from recurrence/reoperation as compared to other materials, depending also on the age of the patients and on the underlying disease (29-32). Main alternative materials are autologous fresh pericardium and, in redo patients with roughened pericardium, substitutes like Photo Fix™ pericardium (Sulzer Carbomedics, Austin, TX, USA) (29) and, particularly for pediatric patients, Core Matrix ECM® (Cormatrix Cardiovascular, Sunnyvale, CA, USA) (12, 29). Our approach is perfectly positioned to extending the study of CET with the use of these materials. Finally, in the event that the use of autologous pericardium is deemed crucial by the surgeon, a pre-cut BPP could be replaced by the use of sterile cutting masks, allowing the surgeon to simply and efficiently obtain properly shaped and sized patches in the OR.

CONCLUSIONS

The CET performed with our novel approach proved to be efficient in restoring valve morphology and functioning *in vitro*. The standardized approach in the leaflet-specific patch selection resulted in a more reproducible and simplified surgical approach, which we believe are key features for allowing wider adoption of reparative surgery of the AV.

Financial Support: Supported by the Foundation for Research in Cardiosurgery (a non-profit organization), Milan, Italy: www.forcardiolab.it.

Conflict of Interest: None declared.

Address for correspondence:
Riccardo Vismara
Department of Electronic
Information and Bioengineering
Politecnico di Milano
Via Golgi 39
20133 Milan, Italy
riccardo.vismara@polimi.it

REFERENCES

1. Cheng A, Dagum P, Miller DC. Aortic root dynamics and surgery: from craft to science. Philos Trans R Soc L. B Biol Sci. 2007;362(1484):1407-1419.
2. Aazami M, Schäfers H-J. Advances in heart valve surgery. J Interv Cardiol. 2003;16(6):535-541.
3. Mangini A, Lemma MG, Soncini M, et al. The aortic interleaflet triangles annuloplasty: a multidisciplinary appraisal. Eur J Cardiothorac Surg. 2011;40(4):851-857.
4. Boodhwani M, de Kerchove L, Glineur D, et al. Repair-oriented classification of aortic insufficiency: impact on surgical techniques and clinical outcomes. J Thorac Cardiovasc Surg. 2009;137(2):286-294.
5. de Kerchove L, Glineur D, Poncelet A, et al. Repair of aortic leaflet prolapse: a ten-year experience. Eur J Cardiothorac Surg. 2008;34(4):785-791.
6. Rahimtoola SH. Choice of prosthetic heart valve in adults an update. J Am Coll Cardiol. 2010;55(22):2413-2426.
7. Hong S, Yi G, Youn Y-N, Lee S, Yoo K-J, Chang B-C. Effect of the prosthesis-patient mismatch on long-term clinical outcomes after isolated aortic valve replacement for aortic stenosis: A prospective observational study. J Thorac Cardiovasc Surg. 2013;146(5):1098-104.
8. Barnett SD, Ad N. Surgery for aortic and mitral valve disease in the United States: a trend of change in surgical practice between 1998 and 2005. J Thorac Cardiovasc Surg. 2009;137(6):1422-1429.
9. Durán CM, Alonso J, Gaite L, et al. Long-term results of conservative repair of rheumatic aortic valve insufficiency. Eur J Cardiothorac Surg. 1988;2(4):217-223.
10. Carr JA, Savage EB. Aortic valve repair for aortic insufficiency in adults: a contemporary review and comparison with replacement techniques. Eur J Cardiothorac Surg. 2004;25(1):6-15.
11. Kalangos A, Beghetti M, Baldovinos A, et al. Aortic valve repair by cusp extension with the use of fresh autologous pericardium in children with rheumatic aortic insufficiency. J Thorac Cardiovasc Surg. 1999;118(2):225-236.
12. Polimenakos AC, Sathanandam S, Blair C, Elzein C, Roberson D, Ilbawi MN. Selective tricuspidization and aortic cusp extension valvuloplasty: outcome analysis in infants and children. Ann Thorac Surg. 2010;90(3):839-846, discussion 846-847.
13. Ahn H, Kim K-H, Kim YJ. Midterm result of leaflet extension technique in aortic regurgitation. Eur J Cardiothorac Surg. 2002;21(3):465-469.
14. Odim J, Laks H, Allada V, Child J, Wilson S, Gjertson D. Results of aortic valve-sparing and restoration with autologous pericardial leaflet extensions in congenital heart disease. Ann Thorac Surg. 2005;80(2):647-653, discussion 653-654.
15. Polimenakos AC, Sathanandam S, Elzein C, Barth MJ, Higgins RSD, Ilbawi MN. Aortic cusp extension valvuloplasty with or without tricuspidization in children and adolescents: long-term results and freedom from aortic valve replacement. J Thorac Cardiovasc Surg. 2010;139(4):933-941, discussion 941.
16. Kunzelman KS, Grande KJ, David TE, Cochran RP, Verrier ED. Aortic root and valve relationships. Impact on surgical repair. J Thorac Cardiovasc Surg. 1994;107(1):162-170.
17. Thubrikar M, Robicsek F. A new aortic root prosthesis with compliant sinuses for valve-sparing operations. Ann Thorac Surg. 2001;71(5)(Suppl 1):S318-S322.
18. Labrosse MR, Beller CJ, Robicsek F, Thubrikar MJ. Geometric modeling of functional trileaflet aortic valves: development and clinical applications. J Biomech. 2006;39(14): 2665-2672.
19. Santibáñez-Salgado JA, Olmos-Zúñiga JR, Pérez-López M, et al. Lyophilized glutaraldehyde-preserved bovine pericardium for experimental atrial septal defect closure. Eur Cell Mater. 2010;19:158-165.
20. de Kerchove L, Vismara R, Mangini A, et al. *In vitro* comparison of three techniques for ventriculo-aortic junction annuloplasty. Eur J Cardiothorac Surg. 2012;41(5):1117-1124.
21. Vismara R, Fiore GB, Mangini A, et al. A novel approach to the *in vitro* hydrodynamic study of the aortic valve: mock loop development and test. ASAIO J. 2010;56(4):279-284.
22. Vismara R, Antona C, Mangini A, et al. *In vitro* study of aortic valves treated with neo-chordae grafts: hydrodynamics and tensile force measurements. Ann Biomed Eng. 2011;39(3):1024-1031.
23. Vismara R, Mangini A, Romagnoni C, Contino M, Redaelli A, Fiore GBAC. *In vitro* study of a porcine quadricuspid aortic valve. J Heart Valve Dis. 2014 [in press].
24. Vismara, Riccardo; Leopaldi, Alberto Maria; Mangini, Andrea; Romagnoni, Claudia; Contino, Monica; Antona, Carlo; Fiore GB. *In vitro* study of the Aortic Interleaflet Triangle Reshaping. J Biomech. 2014;47(2):329-33.
25. Leyh RG, Schmidtke C, Sievers HH, Yacoub MH. Opening and closing characteristics of the aortic valve after different types of valve-preserving surgery. Circulation. 1999;100(21):2153-2160.
26. Sacks MS, Chuong CJ. Orthotropic mechanical properties of chemically treated bovine pericardium. Ann Biomed Eng. 1998;26(5):892-902.
27. Conti CA, Della Corte A, Votta E, et al. Biomechanical implications of the congenital bicuspid aortic valve: a finite element study of aortic root function from *in vivo* data. J Thorac Cardiovasc Surg. 2010;140(4):890-6, 896.e1-2.
28. Della Corte A, Bancone C, Conti CA, et al. Restricted cusp motion in right-left type of bicuspid aortic valves: a new risk marker for aortopathy. J Thorac Cardiovasc Surg. 2012; 144(2):360-9, 369.e1.
29. Myers PO, Tissot C, Christenson JT, Cikirikcioglu M, Aggoun Y, Kalangos A. Aortic valve repair by cusp extension for rheumatic aortic insufficiency in children: Long-term results and impact of extension material. J Thorac Cardiovasc Surg. 2010;140(4):836-844.
30. d'Udekem Y, Siddiqui J, Seaman CS, et al. Long-term results of a strategy of aortic valve repair in the pediatric population. J Thorac Cardiovasc Surg. 2013;145(2):461-467, discussion 461-469.
31. Mayer K, Aicher D, Feldner S, Kunihara T, Schäfers H-J. Repair versus replacement of the aortic valve in active infective endocarditis. Eur J Cardiothorac Surg. 2012;42(1): 122-127.
32. David TE. Aortic valve repair for active infective endocarditis. Eur J Cardiothorac Surg. 2012;42(1):127-128.

APPENDIX A - GEOMETRICAL MODEL

Here we report the strategy to obtain standardized patches of different sizes. This geometrical model was developed to correlate the intercommissural distances, which are simple to evaluate in the OR. These serve as the input to the model, to the free edge lengths, so as to obtain patches suitable to different patient sizes. The coapting height of the patches (Fig. 1c in the paper) was not scaled with the aortic valve diameter, and was fixed to a precautionary value of 6 mm. This choice is coherent with the literature (1-3), and is aimed at ensuring a proper symmetrical coaptation independently of the size of each patch.

Legend

- ID = inter-commissural distances (AC, AB, BC)
- FE = free edge
- Dc = diameter of the circumference passing through the commissures
- O = center of Dc
- O' = coaptation center
- O" = projection of the coaptation center O' on the commissural plane
- d = distance between the commissural plane and the coaptation plane
- AO'B, AO'C, BO'C = segments composing the Fes
- AO"B, AO"C, BO"C = projections of the FE segments on the commissural plane
- Φ_A, Φ_B, Φ_C = angles between the three commissure and the FEs

Assumptions

- The commissures lie on a plane that is parallel to the annular plane (4).
- The projection of the AV coaptation center on the commissural plane coincides with the incenter of the scalene triangle having the three commissures as vertex.
- The distance between the commissural plane and the annular plane is calculated using an equilateral commissural triangle with a free edge angle of 32° (5, 6).

GEOMETRICAL MODEL

The aim of the model is to calculate the length of the three FEs of the aortic valve, given the three IDs as input. In this way, when performing CET, the surgeon can measure the three IDs with compasses and get an indication of the sizes of the pre-cut patches to be implanted on the leaflets.

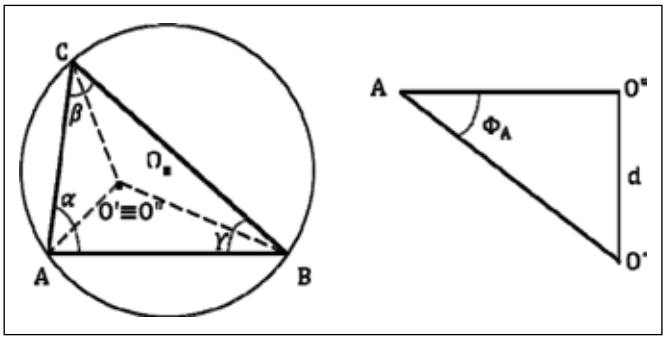

Fig. 1 - ***Left.*** *Geometrical scheme of the aortic valve projected on the commissural plane.* ***Right.*** *View of the angle between the leaflet FE and the commissural plane.*

The FE length can be calculated, for each leaflet, as the sum of the two segments connecting the commissure and the valve coaptation center:

$$FE_{AB} = \overline{AO'} + \overline{BO'} \quad [1]$$

$$FE_{BC} = \overline{BO'} + \overline{CO'} \quad [2]$$

$$FE_{CA} = \overline{CO'} + \overline{AO'} \quad [3]$$

Given the three IDs that the surgeon can measure in the OR, it is possible to calculate the diameter of the commissural circumference Dc using the following expression, valid for every triangle:

$$D_c = \frac{\overline{AB}\,\overline{BC}\,\overline{CA}}{2S} \quad [4]$$

Where S is the area of the triangle ABC, which can be calculated using the Erone formula:

$$S = \sqrt{p(p-\overline{AB})\,(p-\overline{BC})\,(p-\overline{CA})} \quad \text{where} \quad p = \frac{\overline{AB}+\overline{BC}+\overline{CA}}{2} \quad [5]$$

In order to calculate the distance between the commissural plane and the coaptation center plane, we assume that the coaptation plane of the scalene valve coincides with that of an equilateral valve having the same Dc. Several studies have demonstrated that the angle Φ between the commissural plane and the FE is around 32° (5, 6). Hence, the distance d can be easily calculated as follows:

$$d = \frac{D_c}{2}\sin 32 \quad [6]$$

The projection of the three segments composing the FEs (AO", BO", CO") on the commissural plane can be calculated using the cosine theorem:

$$\overline{AO"} = \frac{\sin\left(\frac{\gamma}{2}\right)}{\sin\left(\frac{\gamma}{2}+\frac{\alpha}{2}\right)}\overline{AB} \quad [7]$$

$$\overline{BO"} = \frac{\sin\left(\frac{\alpha}{2}\right)}{\sin\left(\frac{\gamma}{2}+\frac{\alpha}{2}\right)}\overline{AB} \quad [8]$$

$$\overline{CO"} = \frac{\sin\left(\frac{\alpha}{2}\right)}{\sin\left(\frac{\beta}{2}+\frac{\alpha}{2}\right)}\overline{CA} \quad [9]$$

Where the three angles can be calculated using the Carnot theorem:

$$\frac{\alpha}{2} = \frac{1}{2}\cos^{-1}\frac{\overline{CA}^2 + \overline{AB}^2 - \overline{BC}^2}{2\overline{CA}\ \overline{AB}} \quad [10]$$

$$\frac{\beta}{2} = \frac{1}{2}\cos^{-1}\frac{\overline{CA}^2 + \overline{BC}^2 - \overline{AB}^2}{2\overline{CA}\ \overline{BC}} \quad [11]$$

$$\frac{\gamma}{2} = \frac{1}{2}\cos^{-1}\frac{\overline{AB}^2 + \overline{BC}^2 - \overline{CA}^2}{2\overline{AB}\ \overline{BC}} \quad [12]$$

The three angles between the commissural plane and the FEs can be calculated as follows:

$$\varphi_A = \tan^{-1}\frac{d}{\overline{AO"}} \quad [13]$$

$$\varphi_B = \tan^{-1}\frac{d}{\overline{BO"}} \quad [14]$$

$$\varphi_C = \tan^{-1}\frac{d}{\overline{CO"}} \quad [15]$$

Hence, with reference to Equations 1, 2, and 3, the three segments composing the FEs can be calculated as:

$$\overline{AO'} = \frac{\overline{AO"}}{\cos\varphi_A} \quad [16]$$

$$\overline{BO'} = \frac{\overline{BO"}}{\cos\varphi_B} \quad [17]$$

$$\overline{CO'} = \frac{\overline{CO"}}{\cos\varphi_C} \quad [18]$$

REFERENCES

1. Kalangos A, Beghetti M, Baldovinos A, et al. Aortic valve repair by cusp extension with the use of fresh autologous pericardium in children with rheumatic aortic insufficiency. J Thorac Cardiovasc Surg. 1999;118(2):225-236.
2. Polimenakos AC, Sathanandam S, Blair C, Elzein C, Roberson D, Ilbawi MN. Selective tricuspidization and aortic cusp extension valvuloplasty: outcome analysis in infants and children. Ann Thorac Surg. 2010;90(3):839-846; discussion 846-7.
3. Ahn H, Kim K-H, Kim YJ. Midterm result of leaflet extension technique in aortic regurgitation. Eur J Cardiothorac Surg. 2002;21(3):465-469.
4. Labrosse MR, Beller CJ, Robicsek F, Thubrikar MJ. Geometric modeling of functional trileaflet aortic valves: development and clinical applications. J Biomech. 2006;39(14): 2665-2672.
5. Swanson M, Clark RE. Dimensions and geometric relationships of the human aortic valve as a function of pressure. Circ Res. 1974;35(6):871-882.
6. Thubrikar M, Piepgrass WC, Shaner TW, Nolan SP. The design of the normal aortic valve. Am J Physiol. 1981;241(6): H795-801.